Hyperfine Interact (2007) 174:83–88
DOI 10.1007/s10751-007-9568-6

Hot electron plasmas trapped in helical magnetic surfaces

H. Himura · H. Wakabayashi · Y. Yamamoto · A. Sanpei · S. Masamune · M. Isobe · S. Okamura · K. Matsuoka

Published online: 3 July 2007

Abstract Experimental studies on nonneutral (pure electron) plasmas of finite temperature, trapped in helical closed magnetic surfaces have been conducted. The helical electron plasmas are produced with thermal electrons launched from the outside of the last closed flux surface (LCFS). About 150 μs after the electron injection, the plasmas reach equilibrium state. Around the LCFS, a steep gradient of plasma space potential ϕ_s is formed. The corresponding radial electric field is about 2.5 kV/m. On the other hand, around the magnetic axis of helical magnetic surfaces, ϕ_s is almost constant, indicating that there are little electrons there. The volume-averaged electron density is on the order of 10^{13} m^{-3}, smaller than the Brillouin density limit. The confinement time seems to be limited by a disruptive instability, and is so far about 1.5 ms.

Keywords Toroidal nonneutral plasmas · Helical magnetic surfaces

PACS 52.27.Jt · 52.27.Aj · 52.55.Hc · 52.70.Ds

1 Introduction

While nonneutral plasmas trapped in purely toroidal magnetic fields have been studied intensively for five decades [1], nonneutral plasmas confined in toroidal magnetic surfaces without any electric fields have just been investigated [2, 3]. The method of confining electrically nonneutral plasmas in closed magnetic surfaces

H. Himura (✉) · Y. Yamamoto · A. Sanpei · S. Masamune
Department of Electronics, Kyoto Institute of Technology, Kyoto 606-8585, Japan
e-mail: himura@kit.ac.jp

H. Wakabayashi · M. Isobe · S. Okamura · K. Matsuoka
National Institute for Fusion Science, Gifu 509-5292, Japan
e-mail: isobe@nifs.ac.jp

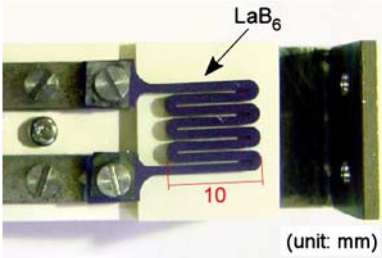

Fig. 1 A picture of the LaB_6 emitter

offers a possibility of reproportioning electrons and ions inside magnetic surfaces because the field is completely closed. This property may be applied to produce various fascinating plasmas such as two-fluid plasmas or electron-positron plasmas which have been studied mainly theoretically. The Compact Helical System (CHS) machine [4] is one of middle-sized stellarator devices for fusion plasmas, which can thus precisely form helical magnetic surfaces. A schematic drawing of CHS can be found in [4, 5]. Using the machine, we have studied helical nonneutral plasmas having hot electron temperature T_e up to $\sim$ 250 eV. In order to produce the plasma on CHS, thermal electrons have been injected via stochastic magnetic layer [5, 6]. Large space potential of the produced helical nonneutral plasma has been measured with a high-impedance emissive probe [7]. At the first series of experiments, we have successfully produced hot helical nonneutral plasmas on CHS. In this contributed paper, we present experimental results on basic properties of CHS helical nonneutral (electron) plasmas.

2 Properties of helical electron plasmas on CHS

Experiments have been conducted on CHS whose major R and average minor radii $\bar{r}$ are 1.0 and 0.2 m, respectively. The key parameter which identifies the configuration is the magnetic axis R_{ax} that is usually fixed at R = 101.6 cm. For this case, the stochastic magnetic region (SMR) [5, 6] is present where the LCFS is completely detached from the vacuum chamber. Thus, helical magnetic surfaces are electrically isolated. The typical magnetic field strength B is 0.9 kG at R_{ax}, which yields $\rho_e \sim$ 1.3 mm when the maximum speed of electrons is $v_e \sim 2 \times 10^7$ m/s for $eV_{acc} \sim 1.2$ keV, where ρ_e, v_e, and eV_{acc} are the Larmor radius, the electron velocity, and the beam energy, respectively.

Electrons are injected from a diode-type electron gun (henceforth called e-gun) which uses a LaB_6 emitter as the cathode. Figure 1 shows a picture of the LaB_6 emitter. Values of beam current (I_b) and eV_{acc} of the injected electrons can be varied. The e-gun is installed in the equatorial plane at $z = 0$ and the cathode is placed in the SMR, usually at $r \sim 117.5$ cm which is about 2 cm outside the LCFS. Nevertheless, substantial penetration of the injected electrons is observed in $\sim 100\ \mu$s [5, 6] and helical electron plasmas are produced inside magnetic surfaces.

2.1 Plasma space potential ϕ_s

Plasma space potential ϕ_s are measured with the high-impedance emissive probe, and the data can be obtained at two different cross sections along the r and z axes on

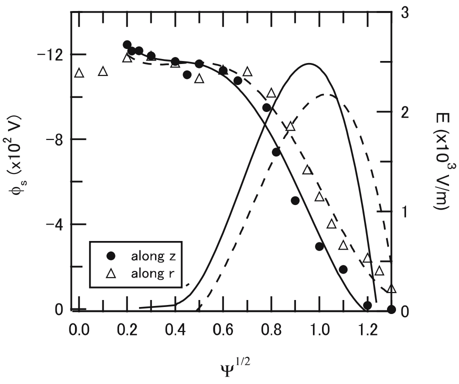

Fig. 2 A typical data of $\phi_s(r)$ and $\phi_s(z)$ for the case of V_{acc} = 1.2 kV. The *solid* and *dashed curves* correspond to E_z and E_r calculated from $E_\alpha = -\nabla_\alpha \phi_s(\alpha)$, respectively

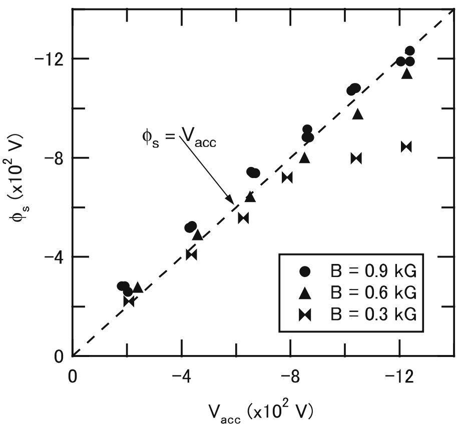

Fig. 3 The maximum ϕ_s at R_{ax} plotted against eV_{acc}

CHS. Here, we use a cylindrical coordinate measured from the center of the torus. Figure 2 shows a typical data of $\phi_s(r)$ and $\phi_s(z)$ for V_{acc} = 1.2 kV. The horizontal axis is shown in $\Psi^{1/2}$ where $\Psi^{1/2} = 0$ and 1 correspond to the R_{ax} and LCFS, respectively. As recognized, large negative potential of ϕ_s is formed in magnetic surfaces. The corresponding electric field E is also depicted in Fig. 2, which indicates that the maximum value of E is about 3 kV/m at LCFS.

The value of ϕ_s achieves its maximum in the neighbourhood of R_{ax}. Figure 3 shows ϕ_s at R_{ax} measured against eV_{acc} for cases of B = 0.9, 0.6, and 0.3 kG. As seen from the plotted data in Fig. 3, ϕ_s increases significantly with V_{acc}. In addition, stronger B results in the larger ϕ_s. These results indicates that the maximum ϕ_s is limited by both eV_{acc} and the strength of B. The dependence on eV_{acc} can roughly be understood by invoking energy conservation for the injected electron. Assuming that the electron drift (rotation) speed is $(-\nabla\phi_s)/B$, it is calculated to be $\sim 10^5$ m/s. As will be shown, this value is much smaller than the electron thermal speed $v_{th}(> 10^6\ m/s)$. Then, $e\phi_s = eV_{acc} - (3\kappa T_e/2) - \omega P \simeq eV_{acc} - (3\kappa T_e/2) \leq eV_{acc}$ [8], where $3\kappa T_e/2$ and ωP are thermal and drift (rotation) energies, respectively. On the other hand, the dependence on B is probably due to better confinement of electrons in the stronger B.

Fig. 4 Typical data of $n_e(z)$ for $B = 0.9$ kG and $V_{acc} =$ 600 V

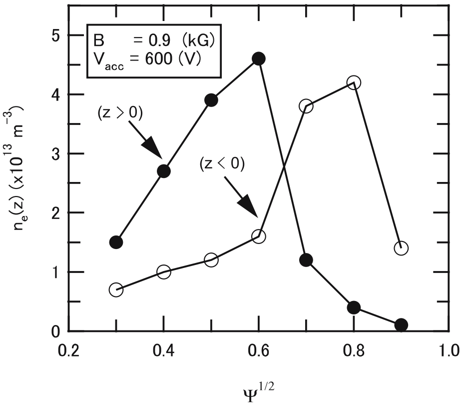

2.2 Electron density n_e and temperature T_e

The current-voltage (I_e-V_p) characteristics are also measured at each magnetic surface using the same emissive probe. Regarding with n_e, it is obtained from I_e ($\sim e n_e v_{th} S$) at $V_p = \phi_s$, where ϕ_s has been pre-measured just before the I_e measurement, where S is the probe area. All other contributions to I_e except v_{th} are ignored, because v_{th} is much faster for the presented hot electron plasmas, as mentioned. Figure 4 shows $n_e(z)$ for B = 0.9 kG and V_{acc} = 600 V. As seen from the plotted data, values of n_e are on the order of 10^{13} m^{-3} in magnetic surfaces. Meanwhile, as explained in Fig. 2, the value of ϕ_s has decreased monotonically at $\Psi^{1/2} \geq 0.7$, that is, near the plasma boundary. Thus, if we apply $\nabla^2\phi_s = e n_e/\epsilon_0$ to the region, the experimental value of n_e is inferred to be 10^{11-13} m^{-3} for $\phi_s \sim 1$ kV, which is consistent with the measured n_e there.

Here, one notes that unlike for fusion plasmas, n_e is non-constant on each magnetic surface. In fact, such a non-uniformity can be recognized also in ϕ_s. Although the detail is now under reviewed [9], these results confirm a fairly recent theoretical prediction [10] on equilibria of toroidal nonneutral plasmas confined in magnetic surfaces. In fact, by a dimensional analysis of the theory, the variation of ϕ_s on magnetic surfaces could be on the same order of T_e/e. Figure 5 shows a preliminary result of $T_e(z)$ for V_{acc} = 600 V and B = 0.9 kG. As seen from the data, T_e is in the range between 40 and 250 eV. The value of T_e approximately corresponds to the observed variations of ϕ_s which are ≤ 150 V. Similar consideration hold also for the $V_{acc} = 1$ kV case in which $T_e \leq 250$ eV and the difference in $\phi_s \leq 350$ V.

2.3 Confinement time τ_N

An estimate of the confinement time τ_N of helical electron plasmas can be obtained from the signal of I_p placed at the LCFS. Typical data are shown in Fig. 6, which indicates that I_p persists for ~ 1.5 ms after the electron injection is turned off at $t \sim 1.4$ ms. Thus, this result infers that τ_N is also about 1.5 ms for this shot. In fact, in most shots, τ_N is limited by a disruptive instability whose spike appears at the end of the duration of I_p, as seen at $t \sim 3$ ms in Fig. 6. Although the details are still

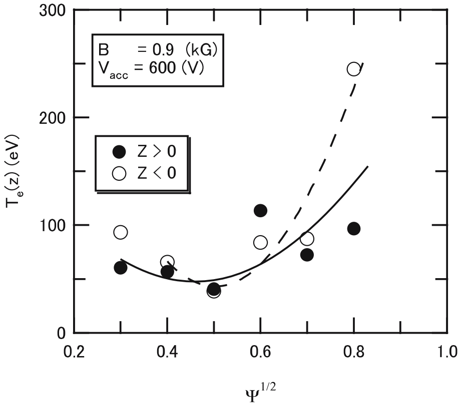

Fig. 5 A preliminary result of $T_e(z)$ for $V_{acc} = 600$ V and $B = 0.9$ kG

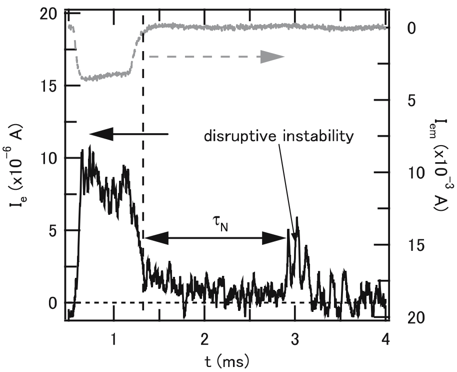

Fig. 6 Typical signals of I_p measured at the LCFS, with the electron injection current from the e-gun

unknown, recent experiments have accumulated many data on the observed spike signals to address the instability of helical nonneutral plasmas.

Finally, since τ_N is approx. 1 ms, the transport coefficient in experiments D_{exp} is calculated to be $\sim \bar{r}/2\tau_N \sim 10$ m^2/s. In most cases of helical neutral plasmas, the dominant transport mechanism is helically trapped particle (HTP) loss [11]. However, this does not account for helical electron plasmas. This is because the speed of HTP can be estimated as $m_e v_{e\perp}^2/(eBR_h) \sim 3 \times 10^4$ m/s, where R_h is the radius of curvature for **B**. Thus, the coefficient D_h due to the HTP loss is approximately $\sim 10^6$ m^2/s, which is too large to explain D_{exp}. On the other hand, the coefficient due to radial electric field D_E [11] is about 10 m^2/s, which seems to be same order as D_{exp}.

Acknowledgements The authors are grateful to the CHS group for performing this research on CHS. This work is performed under auspices of the NIFS CHS Research Collaboration.

References

1. Daugherty, J.D., Eninger, J.E., Janes, G.S.: Experiments on the injection and containment of electron clouds in a toroidal apparatus. Phys. Fluids **12**, 2677 (1969)
2. Nakashima, C., Yoshida, Z., Himura, H., et al.: Injection of electron beam into a toroidal trap using chaotic orbits near magnetic null. Phys. Rev. E **65**, 036409 (2002)

3. Pedersen, T.S.: First non-neutral plasmas in the Columbia non-neutral torus. In: Stellarator news, vol. 99, p. 3 (2005)
4. Nishimura, K., Matsuoka, K., Fujiwara, M., et al.: Compact helical system physics and engineering design. Fus. Technol. **17**, 86 (1990)
5. Himura, H., Wakabayashi, H., Fukao, M., et al.: Observation of collisionless inward propagation of electrons into helical vacuum magnetic surfaces via stochastic magnetic fields. Phys. Plasmas **11**, 492 (2004)
6. Himura, H., Wakabayashi, H., Fukao, M., et al.: Experiments on injecting electrons into helical magnetic field configuration. IEEE Trans. Plasma Sci. **32**, 510 (2004)
7. Himura, H., Fukao, M., Wakabayashi, H., Yoshida, Z.: Filament size of floating-emissive probe for low density plasmas with large space potential. **74**, 4658 (2003)
8. Himura, H., Nakashima, C., Saito, H., Yoshida, Z.: Probing of flowing electron plasmas. Phys. Plasmas **8**, 4651 (2001)
9. Himura, H., Wakabayashi, H., Yamamoto, Y., et al.: Experimental verification of non-contant potential and density on magnetic surfaces of helical nonneutral plasmas. Phys. Plasmas **14**, 022507 (2007)
10. Pedersen, T.S., Boozer, A.H.: Confinement of nonneutral plasmas on magnetics surfaces. Phys. Rev. Lett. **88**, 205002 (2002)
11. Wakatani, M.: Stellarator and heliotron devices, p. 271. Oxford University Press, New York (1998)